Regulation of Ca^{2+} signalling and Ca^{2+}-mediated cell death by the transcriptional coactivator PGC-1α

K Bianchi[1,2,4], G Vandecasteele[1,2,3,4], C Carli[1,2], A Romagnoli[1,2], G Szabadkai[1,2] and R Rizzuto*[,1,2]

[1] Department of Experimental and Diagnostic Medicine, Section of General Pathology, University of Ferrara, Ferrara 44100, Italy
[2] Interdisciplinary Center for the Study of Inflammation (ICSI), University of Ferrara, Ferrara 44100, Italy
[3] Laboratoire de Cardiologie Cellulaire et Moleculaire, INSERM U-446, Universite Paris-Sud, Faculte de Pharmacie, Chatenay-Malabry F-92296, France
[4] These authors contributed equally to this work
* Corresponding author: R Rizzuto, Department of Experimental and Diagnostic Medicine, General Pathology Section, University of Ferrara, Via L. Borsari 46, Ferrara 44100, Italy. Tel: + 39 0532 291361; Fax: + 39 0532 247278; E-mail: r.rizzuto@unife.it

Abstract

Mitochondrial Ca^{2+} uptake controls cellular functions as diverse as aerobic metabolism, cytosolic Ca^{2+} signalling and mitochondrial participation in apoptosis. Modulatory inputs converging on the organelle can regulate this process, determining the final outcome of Ca^{2+}-mediated cell stimulation. We investigated in HeLa cells and primary skeletal myotubes the effect on Ca^{2+} signalling of the transcriptional peroxisome-proliferator-activated-receptor-γ-coactivator-1α (PGC-1α), which triggers organelle biogenesis and modifies the mitochondrial proteome. PGC-1α selectively reduced mitochondrial Ca^{2+} responses to cell stimulation by reducing the efficacy of mitochondrial Ca^{2+} uptake sites and increasing organelle volume. In turn, this affected ER Ca^{2+} release and cytosolic responses in HeLa cells. Most importantly, the modulation of mitochondrial Ca^{2+} uptake significantly reduced cellular sensitivity to the Ca^{2+}-mediated proapoptotic effect of C$_2$ ceramide. These results reveal a primary role of PGC-1α in shaping mitochondrial participation in calcium signalling, that underlies its protective role against stress and proapoptotic stimuli in pathophysiological conditions.
Cell Death and Differentiation (2006) **13,** 586–596.
doi:10.1038/sj.cdd.4401784; published online 21 October 2005

Keywords: mitochondria; calcium; apoptosis; PGC-1α

Abbreviations: ACh, acetylcholine; CCh, carbamylcholine; $[Ca^{2+}]_c$, cytosolic $[Ca^{2+}]$; $[Ca^{2+}]_{er}$, endoplasmic reticulum $[Ca^{2+}]$; $[Ca^{2+}]_m$, mitochondrial $[Ca^{2+}]$; $[Ca^{2+}]_{sr}$, sarcoplasmic reticulum $[Ca^{2+}]$; cytAEQ, cytosolic aequorin; ER, endoplasmic reticulum; erAEQmut, endoplasmic reticulum-targeted mutated aequorin; FCCP, carbonyl cyanide 4-(trifluoromethoxy)phenylhydrazone; IP$_3$, inositol 1,4,5 trisphosphate; IP$_3$R, inositol 1,4,5 trisphosphate receptor; mAchR, muscarinic Ach receptor; mtAEQmut, mitochondrially targeted mutated aequorin; mtGFP, mitochondrially targeted green fluorescent protein; MCU, mitochondrial Ca^{2+} uniporter; PPAR-γ, peroxisome-proliferator-activated-receptor-γ; PGC-1α, peroxisome-proliferator-activated-receptor-γ-coactivator-1α; SERCA, sarco/endoplasmic reticulum Ca^{2+}-ATPase; SR, sarcoplasmic reticulum; srAEQmut, sarcoplasmic reticulum-targeted mutated aequorin; TMRM, tetramethyl-rhodamine-methyl-esther; UCP, uncoupling protein

Introduction

Calcium homeostasis is fundamental for cell metabolism, proliferation, differentiation and cell death, and extensive recent work has revealed a key role of intracellular organelles in its versatile regulation (reviewed in Berridge *et al.*[1]). Elevation of intracellular Ca^{2+} concentration is dependent either on Ca^{2+} influx from the extracellular space through the plasmamembrane, or on Ca^{2+} release from intracellular Ca^{2+} stores, such as the endoplasmic/sarcoplasmic reticulum (ER/SR). Mitochondria are organized in a complex interconnected network all over the cell interior, and thus are able to form contacts with the different sources of Ca^{2+} (for recent reviews see Rizzuto *et al.*[2] and Parekh[3]). These close contacts ensure the uptake of Ca^{2+} into the mitochondrial matrix, leading to three important consequences: (i) mitochondria function as cellular Ca^{2+} buffers, shaping the global cellular Ca^{2+} response;[4] (ii) Ca^{2+} entering into the mitochondrial matrix regulates mitochondrial metabolism;[5] (iii) the extent of mitochondrial Ca^{2+} load is a key determinant of the intrinsic apoptotic pathway, thus controlling cell fate under physiological and pathological conditions.[6]

The composite Ca^{2+} uptake system of the mitochondrial membranes comprises the voltage-dependent anion channel of the outer membrane and the Ca^{2+} uniporter (mitochondrial Ca^{2+} uniporter (MCU)) in the inner membrane.[7,8] Mitochondrial Ca^{2+} uptake is tightly dependent on the potential gradient ($\Delta\Psi_m, \sim -180\,mV$, negative inside) of the inner mitochondrial membrane. In turn, $\Delta\Psi_m$ is determined by the activity of electron transport chain complexes, thus metabolic activity of the mitochondria determines also their Ca^{2+} uptake. Moreover, recent works demonstrated that morphological changes, such as fragmentation of the mitochondrial network also leads to changes of mitochondrial Ca^{2+} uptake through the modification of the spatial pattern of the intramitochondrial Ca^{2+} diffusion.[9,10] Importantly, these changes in mitochondrial morphology are associated with the apoptotic processes[11] and they also modify the cellular sensitivity to Ca^{2+}-mediated apoptotic stimuli such as serum deprivation and oxidative stress (reviewed in Bianchi *et al.*[12]).

Recent studies identified fundamental molecular mechanisms of mitochondrial biogenesis, through the characterization of master genes determining the expression of mitochondrial proteins encoded in the nucleus of the cell

(reviewed in Scarpulla[13] and Puigserver and Spiegelman[14]). Among these, the peroxisome-proliferator-activated-receptor-γ coactivator-1α (PGC-1α) displays several features of remarkable interest. First, by integrating the action of several transcription factors, it orchestrates the cellular response to changes in metabolic needs evoked by a number of physiological and pathological stimuli.[14] Indeed, cold exposure, fasting and exercise were shown to induce PGC-1α in a tissue-specific manner either through β-adrenergic stimulation or by Ca^{2+}/calmodulin-dependent protein kinase activation.[15,16] PGC-1α stimulates mitochondrial biogenesis in concert with the increased expression of nuclear-encoded electron transport chain components, metabolic enzymes, and uncoupling proteins (UCPs[17]). The latter effect includes partial mitochondrial uncoupling/depolarization and accounts for the adaptive thermogenic response in brown fat and skeletal muscle cells.[14] On the other hand, apart from its role in these physiological adaptation processes, recent observations suggest that the loss of function of PGC-1α leads to cellular dysfunction and increased sensitivity to apoptosis. PGC-1α null mice show neurodegenerative symptoms, associated with increased cell death in the striatal region of the brain.[18] Similarly, downregulation of PGC-1α in hypertrophic cardiac failure is responsible for apoptotic cell death of cardiac myocytes.[19,20] These effects might due to impaired mitochondrial function, and imply a strong antiapoptotic effect of the protein. However, the mechanisms linking PGC-1α-induced mitochondrial changes to decreased susceptibility to cell death are unknown.

Altogether, these results prompted us to investigate the role of PGC-1α-induced changes in mitochondrial structure and function, particularly mitochondrial and Ca^{2+} homeostasis and apoptotic sensitivity, in different cellular models. In order to explore PGC-1α-induced changes, we combined population measurements and single cell imaging of organellar Ca^{2+} signals, using the differentially targeted Ca^{2+}-sensitive aequorin and ratiometric pericam probes, respectively. Furthermore, we assessed the role of PGC-1α-induced alteration of Ca^{2+} signalling to Ca^{2+}-dependent and -independent apoptotic stimuli.

Results

PGC-1α induces mitochondrial biogenesis and reduces mitochondrial calcium uptake in skeletal myotubes

To demonstrate the effect of PGC-1α on mitochondrial biogenesis we first used primary cultured rat skeletal myotubes. Primary non-differentiated myoblasts were transfected with PGC-1α, and after 5 days of differentiation overexpression of PGC-1α was verified by immunoblotting (Figure 1a). Immunofluorescence analysis showed a low endogenous level of PGC-1α in myotubes and a specific increase of nuclear staining of transfected cells, identified by coexpressed green fluorescent protein (GFP) (Figure 1b). Further immunoblot analysis of PGC-1α-transfected myotube cultures demonstrated upregulation of PGC-1α target genes, such as nuclear respiratory factor-1 (NRF-1) in the cell nucleus and UCP-2 in mitochondria[21] (see Figure 1a). More-

over, similar alteration of the expression profile of PGC-1α and its target genes could be induced by physiological induction of PGC-1α expression. Since PGC-1α was shown to be induced during adaptive thermogenesis through β-adrenergic stimulation of skeletal muscle to induce heat production,[17] primary myotubes were stimulated for 24 h with salbutamol (1 μM), a selective β₂-adrenergic receptor agonist. Salbutamol treatment led to an ∼3-fold induction of PGC-1α and its target genes NRF-1 (∼4-fold) and UCP-2 (∼2.5-fold), comparable to the ∼2.5-fold increase achieved by its exogenous expression (Figure 1a). Then we applied quantitative 3D digital microscopy[9] to quantify mitochondrial volume in control (mitochondrially targeted green fluorescent protein (mtGFP) transfected) and PGC-1α overexpressing myotubes (cotransfected with mtGFP and PGC-1α, Figure 1c). Mitochondrial volume was imaged and quantified as percentage of the volume occupied by mitochondria (mtGFP-positive voxels in the 3D images), in randomly chosen cubic regions inside myotubes. Mitochondria occupied $16.3 \pm 1.26\%$ of the intracellular volume of control cells, while the volume of mitochondria in PGC-1α overexpressing myotubes was almost doubled (Figure 1d, $26.8 \pm 1.69\%$, $P < 0.01$). Thus, recombinant overexpression of PGC-1α in skeletal myotubes was capable of reproducing the complex phenotypic alteration of mitochondria typically induced by this master gene.

To investigate the consequences of these alterations on Ca^{2+} signalling, we carried out a series of experiments using specifically targeted aequorin probes: mitochondrially targeted mutated aequorin (mtAEQmut) for mitochondria, cytosolic aequorin (cytAEQ) for the cytosol, sarcoplasmic reticulum-targeted mutated aequorin (srAEQmut) for the SR.[22] Myotubes were stimulated with carbamylcholine (CCh, 500 μM) that acts on nicotinic acetylcholine (ACh) receptor of myotubes to induce Ca^{2+} influx and trigger Ca^{2+}-induced Ca^{2+} release from the SR. CCh was applied in the presence of the muscarinic ACh receptor (mAChR) blocker atropine (10 μM), in order to exclude any confounding effect of a mAChR response of the fibroblasts present in the cell culture. CCh stimulation caused a robust mitochondrial Ca^{2+} transient in control myotubes (peak value 121.7 ± 15.8 μM), in agreement with previous results.[23] Interestingly, the maximal mitochondrial ($[Ca^{2+}]_m$) response was attenuated by almost 50% in PGC-1α-overexpressing myotubes (63.2 ± 7.6 μM, $P < 0.01$ versus control, Figure 2a). Similarly, β₂-adrenergic receptor-driven induction of PGC-1α expression by salbutamol led to a reduction of mitochondrial Ca^{2+} uptake (83.31 ± 7.28 versus 106 ± 1.7 μM in controls, $P < 0.05$, Figure 2b). In contrast, the elevation of cytosolic $[Ca^{2+}]$ ($[Ca^{2+}]_c$) in response to CCh was not changed in PGC-1α-overexpressing cells (1.77 ± 0.09 μM) as compared to controls (1.85 ± 0.07 μM, Figure 2c), indicating a selective alteration of mitochondrial Ca^{2+} handling. In agreement with these results, the state of filling of the SR showed no difference in PGC-1α-overexpressing cells (steady-state sarcoplasmic reticulum $[Ca^{2+}]$ ($[Ca^{2+}]_{sr}$) values of 295.0 ± 19.8 μM in controls versus 292.2 ± 38.8 μM in PGC-1α-overexpressing cells, Figure 2d). Similarly, the rate of Ca^{2+} leak from the SR, as measured by inhibiting sarco/endoplasmic reticulum Ca^{2+}-ATPase (SERCA) pumps with 100 μM tert-butylhydroquinone (tBHQ) remained unchanged
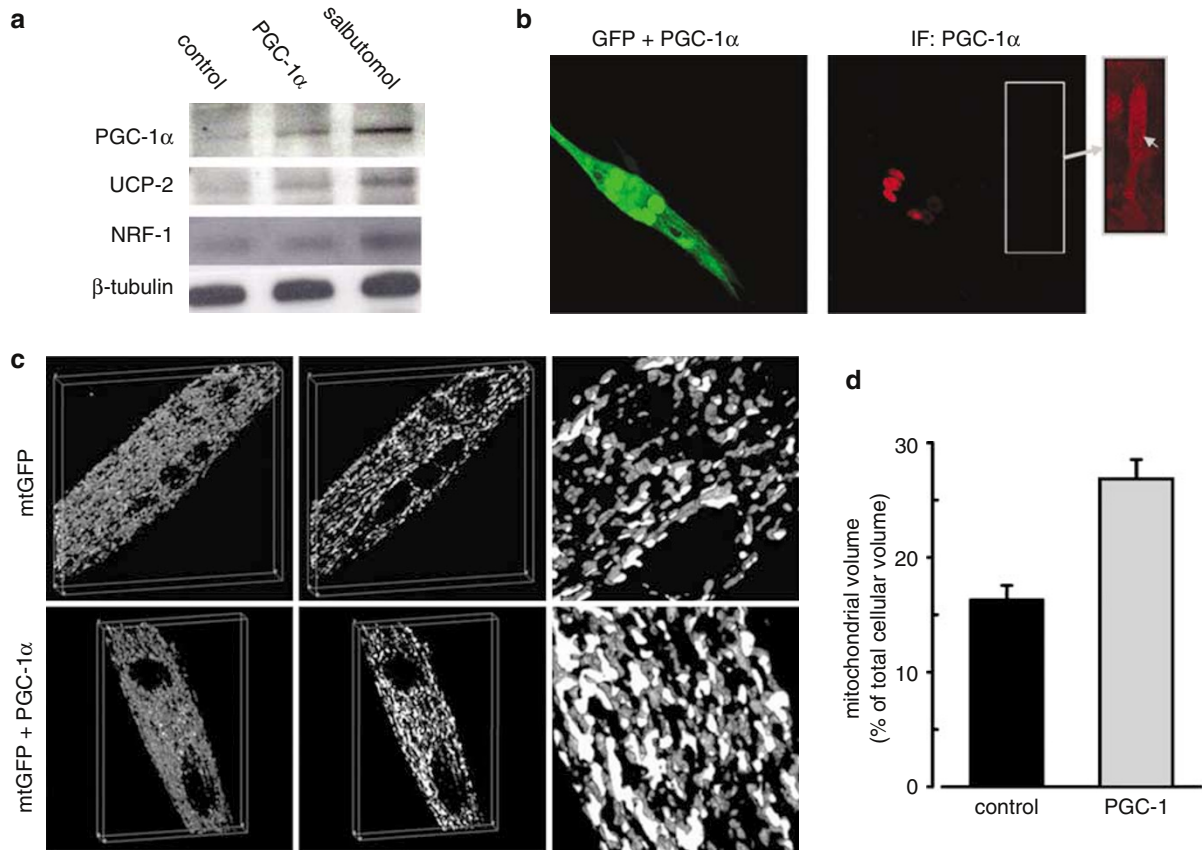
Figure 1 Mitochondrial biogenesis in PGC-1α overexpressing primary skeletal myotubes. (**a**) Western blot analysis of PGC-1α, UCP-2 and NRF-1 expression in control, PGC-1α transfected and salbutamol-treated myotubes (1 μM, 24 h). Total protein extracts (10 μg protein/lane) of primary myotube cultures (7 days after transfection and differentiation) were separated by SDS-PAGE and visualized by immunoblotting as described in Materials and Methods. (**b**) Immunofluorescence analysis of endogenous and exogenously expressed PGC-1α in myotubes. Cells were cotransfected with GFP (left panel) and PGC-1α (immunofluorescence on right panel). Inset shows the nonspecific signal and the low level of expression of endogenous PGC-1α in the nucleus (arrow). (**c**) For mitochondrial morphology analysis, cells were transiently transfected with mtGFP (control, black bars on **b**) or mtGFP + PGC-1α (PGC-1α overexpressing cells, grey bars on **b**). Images acquired by digital microscopy were deconvolved, 3D reconstructed and quantitatively analysed (see Materials and Methods). Representative 3D reconstructed images of control (upper panels) and PGC-1α overexpressing myotubes (lower panels) showing PGC-1α-induced mitochondrial biogenesis. Images of the total (left), Z-clipped (middle) and enlarged Z-clipped (right) mitochondrial volume are shown. The saturated white pixels represent the plane of Z-clipping. (**d**) Effect of PGC-1α overexpression on total organelle volume. Data were obtained from more than 10 cells examined from three separate experiments (P<0.01)

(Figure 2d). Mitochondrial Ca²⁺ uptake was similarly reduced after direct stimulation of RyRs with 20 mM caffeine (93.7±20.8 μM in controls *versus* 56.0±8.8 μM in PGC-1α-overexpressing cells), showing that the effect of PGC-1α was due to the modification of Ca²⁺ signal transmission from the SR to mitochondria. These results show that both physiological induction and exogenous expression of PGC-1α lead to mitochondrial biogenesis coupled to deregulation of mitochondrial Ca²⁺ uptake.

PGC-1α modifies the inositol 1,4,5-trisphosphate (IP₃) receptor (IP₃R)-driven mitochondrial Ca²⁺ signal and consequently Ca²⁺ release from ER and cytosolic Ca²⁺ elevation

To evaluate the mechanism by which PGC-1α changes mitochondrial Ca²⁺ uptake, we tested whether the same effect of PGC-1α could be observed during IP₃-mediated Ca²⁺ signalling in Hela cells. Immunoblot analysis showed

that transient transfection of PGC-1α resulted in an ∼2-fold increase in PGC-1α protein, and in the induction of its target genes, NRF-1 and UCP-2, as observed in primary myoblasts (Figure 3a). Immunofluorescence experiments showed that PGC-1α was located to the nucleus in control and transfected HeLa cells (Figure 3b). Notably however, the endogenous expression of PGC-1α was higher in HeLa cells with respect to primary cultured myotubes (compare Figure 3a and b with Figure 1a and b). Next, we examined mitochondrial morphology and histamine-induced Ca²⁺ signalling following transient overexpression of PGC-1α in HeLa cells. We carried out 3D quantitative imaging of mtGFP-transfected HeLa cells (controls) and of cells cotransfected with mtGFP and PGC-1α (PGC-1α-overexpressing cells), as described above. The results demonstrated that PGC-1α induces mitochondrial biogenesis also in this cell type, although to a lesser extent than in the primary myotubes. As shown in Figure 3c, mitochondria occupied 32.2±5.0% of the volume of control cells, while in PGC-1α-overexpressing cells the mitochondrial volume increased by about 1.65 times (to 40.0±6.0% of
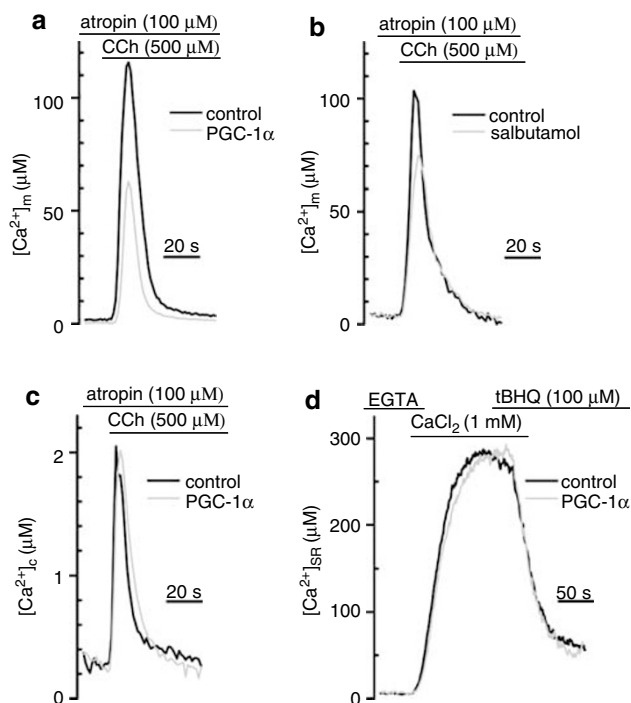
Figure 2 PGC-1α-induced mitochondrial biogenesis in primary skeletal myotubes specifically reduces agonist-induced mitochondrial Ca^{2+} uptake. $[Ca^{2+}]$ measurements in mitochondria (**a** and **b**: mtAEQmut), in the cytosol (**c**: cytAEQ) and in the sarcoplasmic reticulum (**d**: srAEQmut) of primary skeletal myotubes transfected with specifically targeted aequorin probes. Control cells were transfected only with the recombinant Ca^{2+} probe of interest (black traces), or cotransfected with PGC-1α (grey traces in **a**, **c** and **d**). In (**b**), PGC-1α expression was induced by stimulation of skeletal myotubes with the β_2-adrenergic agonist salbutamol (1 μM for 24 h, grey traces). Aequorin luminescence was measured in a population of transfected cells seeded on gelatin-coated coverslips, perfused at 37°C with KRB/Ca^{2+}, and luminescence data were converted to $[Ca^{2+}]$ (see Materials and Methods). Cells were stimulated with CCh (500 μM) where indicated, in the presence of the mAchR blocker atropine (100 μM). In (**d**), skeletal myotubes were transected with srAEQmut alone (control, black traces) or cotransfected with PGC-1α (grey traces). Ca^{2+} (1 mM) was added to induce refilling of the SR followed by tBHQ (100 μM) addition in order to measure the Ca^{2+} leak, after blocking the SERCA pumps. Data are representative of $\geqslant$12 traces obtained from at least three separate experiments

cellular volume, $P<0.01$ versus controls). This reduced effect on mitochondrial volume might be related to the higher endogenous expression of PGC-1α, and may represent a common feature of tumour cell lines since a similar small increase of mitochondrial volume was found in CHO cells (28.2$\pm$2% in mtGFP-expressing controls versus 35.4$\pm$3% in mtGFP/PGC-1α-cotransefected cells, $P<0.05$).

The effect of PGC-1α overexpression on mitochondrial Ca^{2+} accumulation was then investigated. Application of the IP₃ mobilizing agonist histamine (100 μM) to control HeLa cells induced a robust elevation in $[Ca^{2+}]_m$ (peak value: 111.4$\pm$13.2 μM), while in cells overexpressing PGC-1α the same stimulus elicited a markedly lower mitochondrial Ca^{2+} accumulation (peak value: 69.9$\pm$4.9 μM, $P<0.01$ versus control, Figure 3d). These experiments showed that the primary effect of PGC-1α-induced mitochondrial biogenesis on the mitochondrial Ca^{2+} uptake rely on the organelle itself, independently of the source of Ca^{2+} signal.

Since mitochondrial Ca^{2+} uptake and IP₃-induced Ca^{2+} release from the ER are tightly coupled, we investigated whether the observed changes in mitochondrial Ca^{2+} uptake was accompanied by alterations in cytosolic and ER Ca^{2+} signals. As measured in cell population with the cytAEQ probe, the amplitude of $[Ca^{2+}]_c$ elevation in response to 100 μM histamine was slightly, but consistently reduced in PGC-1α-overexpressing cells. The peak value in controls transfected with cytAEQ was 2.25$\pm$0.09 μM, while in PGC-1α-overexpressing cells, cotransfected with PGC-1α and cytAEQ was 1.98$\pm$0.09 μM ($P<0.05$, Figure 3e). Importantly, after 10 min preincubation with the mitochondrial uncoupler carbonyl cyanide 4-(trifluoromethoxy)phenylhydrazone (FCCP, 10 μM), PGC-1α overexpression had no effect on $[Ca^{2+}]_c$ (peak value in controls: 1.57$\pm$0.1 μM; in PGC-1α-overexpressing cells: 1.7$\pm$0.1 μM). Since the mitochondrial depolarization induced by FCCP completely abolishes mitochondrial Ca^{2+} uptake, these results indicate that the observed reduction in the $[Ca^{2+}]_c$ response was the consequence of PGC-1α-induced reduction of mitochondrial Ca^{2+} accumulation.

We assumed that the observed reduction of the histamine-induced $[Ca^{2+}]_c$ signal in PGC-1α-overexpressing cells might depend on the reduction of Ca^{2+} release from the IP₃-sensitive ER Ca^{2+} store. Thus, we analysed the steady-state ER $[Ca^{2+}]$ ($[Ca^{2+}]_{er}$) levels and the kinetics of histamine-induced Ca^{2+} release from the ER Ca^{2+} store in ER-targeted mutated aequorin (erAEQmut) (control) and erAEQmut and PGC-1α-overexpressing cells. This series of experiment was carried out at low extracellular $[Ca^{2+}]$ (150 μM) and submaximal histamine stimulation (10 μM) to further resolve the kinetics of Ca^{2+} movements. PGC-1α overexpression did not change either the Ca^{2+} uptake rate or the steady-state $[Ca^{2+}]_{er}$ level (control 230$\pm$7.6 μM versus PGC-1α: 228$\pm$9.4 μM, Figure 4c). In contrast, after stimulation with histamine we observed a significant reduction of the maximal Ca^{2+} release velocity of the response (controls: 31.1$\pm$2.2 μM/s, PGC-1α: 23.3$\pm$2.3 μM/s, $P<0.05$, Figure 4a and b).

Based on the above data we supposed that reduced mitochondrial Ca^{2+} uptake during fast Ca^{2+} release from the ER might be a result of the Ca^{2+}-mediated negative feedback on the IP₃R as mitochondria fail to rapidly clear the high $[Ca^{2+}]$ microdomain in proximity of the ER. To further investigate this possibility we applied fast imaging of the cytosolic Ca^{2+} transient in single cells loaded with fura-2. These measurements demonstrated that the kinetics of the initial (<1 s) $[Ca^{2+}]_c$ rise in PGC-1α-overexpressing cells show indeed a faster initial $[Ca^{2+}]_c$ accumulation (maximal speed at $\sim$200 ms after histamine application 0.28$\pm$0.03 dR/s, Figure 4d and e) as compared to the control cells (0.19$\pm$0.03 dR/s, peak velocity at $\sim$300 ms; $P<0.05$). However, in PGC-1α-overexpressing cells the $[Ca^{2+}]_c$ transient terminated earlier, due to the more potent Ca^{2+} inhibition on the Ca^{2+} release, leading to reduced average cytosolic Ca^{2+} response (Figure 4d, see also cytAEQ measurements, Figure 3e). This reduction reflects the inhibition of IP₃-mediated Ca^{2+} release, and match with the results obtained at lower time resolution with the ER-targeted aequorin probe (Figure 4a). We thus conclude that PGC-1α decreases the
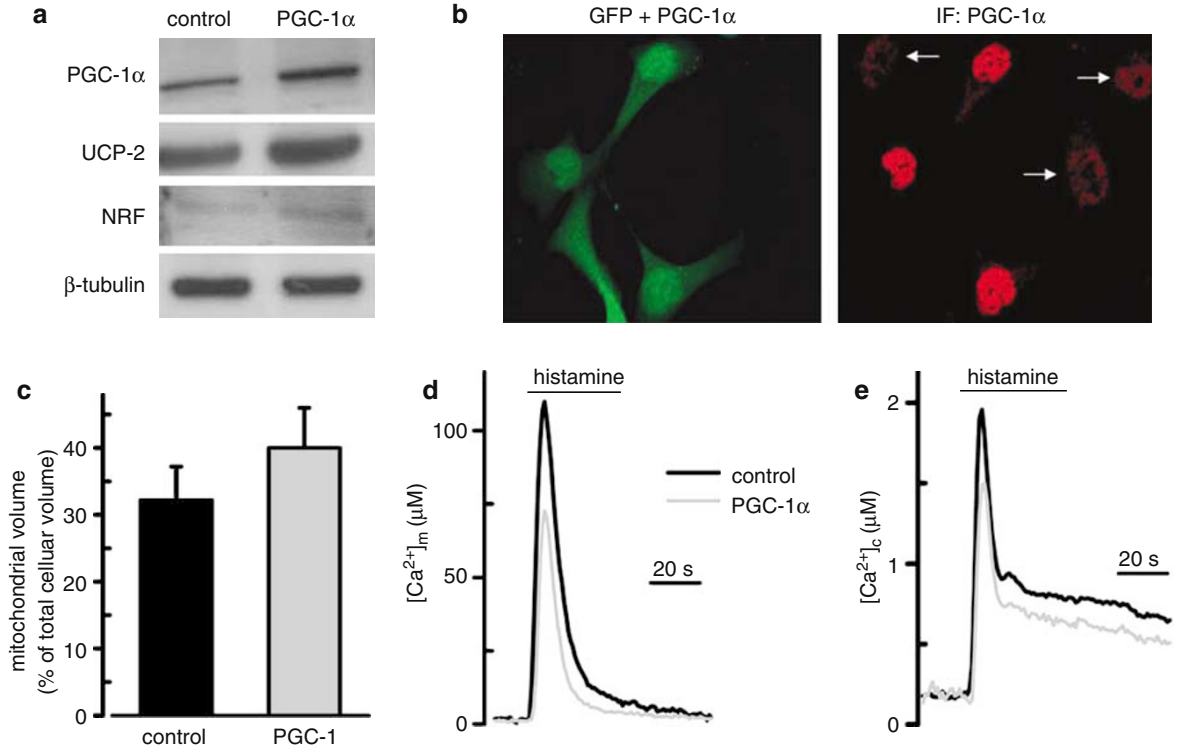
Figure 3 PGC-1α-induced mitochondrial biogenesis in HeLa cells modifies the IP$_3$ receptor-driven mitochondrial Ca^{2+} signal and consequently cytosolic Ca^{2+} elevation. (**a**) Western blot analysis of PGC-1α, NRF-1 and UCP-2 expression in control and PGC-1α-transfected HeLa cells. Total protein extracts (10 μg protein/lane, 36 h after transfection) were separated by SDS-PAGE and visualized by immunoblotting as described in Materials and Methods. (**b**) Immunofluorescence analysis of endogenous and exogenously expressed PGC-1α in HeLa cells. Cells were cotransfected with GFP (left panel) and PGC-1α (immunofluorescence on right panel). Arrows show endogenous PGC-1α in nontransfected cell nuclei. (**c**) Quantitative analysis of mitochondrial network volume in PGC-1α overexpressing HeLa cells. Cells were transiently transfected with mtGFP (control, black bars) or mtGFP + PGC-1α (PGC-1α overexpressing cells, grey bars). Images acquired by digital microscopy were deconvolved, 3D reconstructed and quantitatively analysed (see Materials and Methods). Data were obtained from 10 cells examined from three separate experiments ($P < 0.01$). (**d** and **e**) [Ca^{2+}] measurements in the mitochondrial (**d**: mtAEQmut) and cytosolic (**e**: cytAEQ) compartments of HeLa cells transfected with the respective targeted aequorin probes. Cells were transfected with the aequorin probe (controls, black traces), or cotransfected with PGC-1α (grey traces). Aequorin luminescence was measured and calibrated as in Figure 2 (see also Materials and Methods). Data are representative of ≥ 12 traces obtained from three separate experiments

efficiency of ER-mitochondrial Ca^{2+} signal transmission through the reduction of mitochondrial Ca^{2+} uptake.

PGC-1α reduces Ca^{2+} concentration reached in mitochondria through direct and indirect mechanisms

In order to investigate the mechanism by which PGC-1α exerts its effect on [Ca^{2+}]$_m$ we carried out digital imaging of the mitochondrially targeted ratiometric pericam (2mtRP).[9] This method allowed the quantitative analysis of (i) the initial Ca^{2+} uptake (hot spots), representative of Ca^{2+} uniporter activity in the high [Ca^{2+}] microdomains of ER Ca^{2+} release sites, and (ii) the average distance of the subsequent intramitochondrial Ca^{2+} diffusion, representing the volume in which intramitochondrial Ca^{2+} is distributed. First, we compared the kinetics of Ca^{2+} uptake (Figure 5b, upper panel) after 100 μM histamine stimulation in control (transfected with 2mtRP) and PGC-1α-overexpressing (2mtRP + PGC-1α transfected) cells. Mitochondria of PGC-1α-over-expressing cells showed slower Ca^{2+} uptake kinetics, and reduced maximal mitochondrial Ca^{2+} response (Figure 5b,

upper panel), confirming the results obtained in population measurements using the mtAEQmut probe (see Figure 3d). Then, in the same cells, we analysed the number of active Ca^{2+} uptake sites and the area of Ca^{2+} diffusion. These results showed that (i) the reduction in the initial Ca^{2+} uptake kinetics was due to the reduced number of Ca^{2+} uptake sites in PGC-1α-overexpressing cells (Figure 5b, middle panel), reflecting reduced Ca^{2+} uniporter activity at time points <1 s after stimulation; (ii) diffusion of Ca^{2+} waves to a longer distance during the peak phase of the mitochondrial Ca^{2+} response (after >2 s of histamine application, Figure 5b, lower panel) was responsible for the reduction of maximal [Ca^{2+}]$_m$ achieved during cell stimulation.

Thus, we assumed two mechanisms to explain the effect of PGC-1α on mitochondrial Ca^{2+} handling: (i) PGC-1α directly reduces the driving force and/or inhibits the channel(s) responsible for mitochondrial Ca^{2+} uptake, and (ii) the increased mitochondrial volume in PGC-1α-overexpressing cells allows intramitochondrial Ca^{2+} to distribute in a larger volume, resulting in reduced overall [Ca^{2+}]$_m$ increase during mitochondrial Ca^{2+} accumulation.

To further analyse the mechanism of direct inhibition of mitochondrial Ca^{2+} uptake by PGC-1α we considered that the
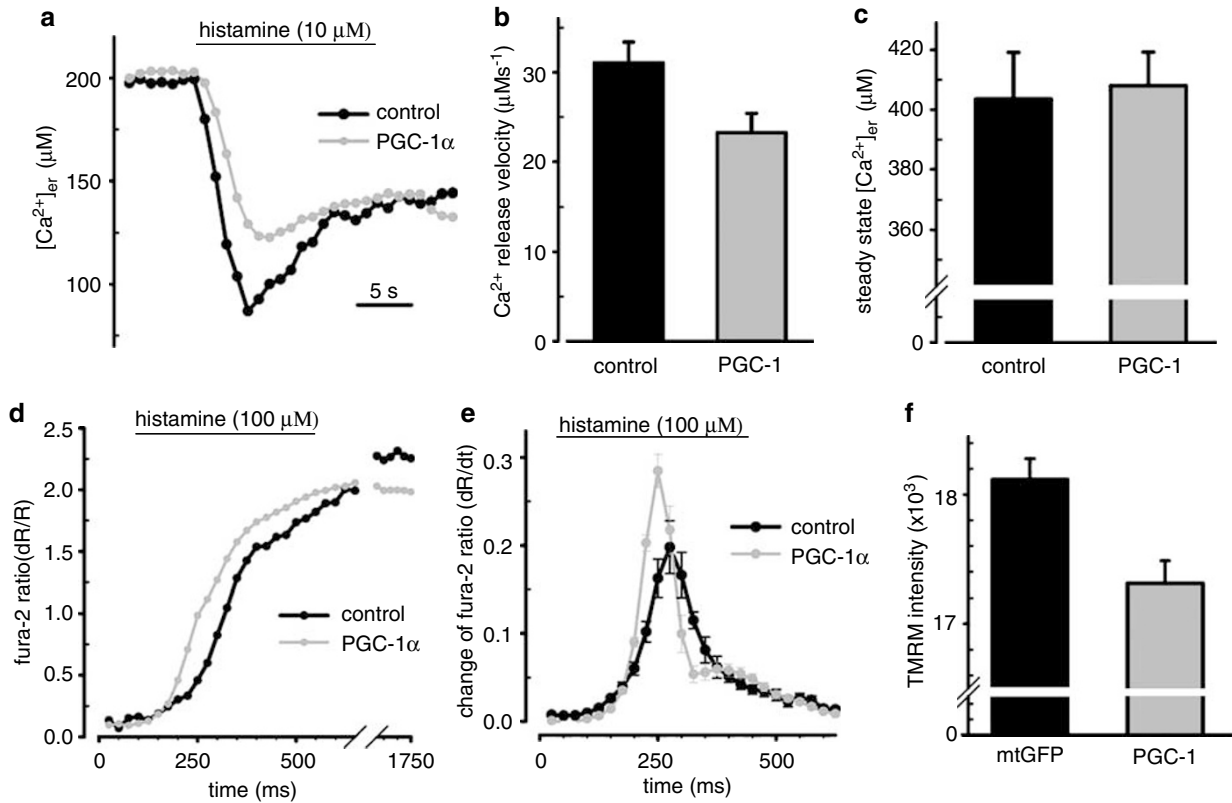
Figure 4 Consequences of PGC-1α overexpression on global Ca²⁺ signals in HeLa cells. (a–c) [Ca²⁺]$_{er}$ was measured in HeLa cells transfected with erAEQmut (control, black traces) or cotransfected with PGC-1α (grey traces). Cells were reconstituted with coelenterazine in KRB/EGTA solution, then Ca²⁺ (150 μM) was added to induce refilling of the ER. Ca²⁺ release was induced by the addition of histamine (10 μM) (a). Velocity of histamine-induced Ca²⁺ release from the ER (controls: black bar; PGC-1α-overexpressing cells: grey bar) (b). [Ca²⁺]$_{er}$ values at steady-state ER Ca²⁺ filling (controls: black bar; PGC-1α-overexpressing: grey bar) (c). Data are representative of ≥12 traces, $P < 0.05$. (d and e) Fast imaging of the cytosolic Ca²⁺ transient in fura-2-loaded single HeLa cells. Hela cells were transfected with pHcRed (control: black trace) or cotransfected with PGC-1α (grey trace). Excitation ratio (340/380 nm) was calculated after background subtraction and average values of individual cells were normalized to the initial R-values (dR/R) (d). Then, the series of 340/380 nm excitation ratio images were temporally derived, and the actual velocity of [Ca²⁺] changes, averaged for each cell, were calculated (e). Panel d illustrates representative dR/R traces, while the traces in panel e are the mean velocity (± S.E.M.) of ≥25 single cell measurements from three separate experiments. (f) Steady-state TMRM fluorescence intensity values measured in mtGFP (control, black bar) and mtGFP + PGC1α (grey bar)-transfected cells. Cells were loaded at 37°C for 30 min with 20 nM TMRM, then Z-series images were taken by confocal microscopy (see Materials and Methods). Values were calculated from individual cells ($n ≥ 250$; $P < 0.01$) after background subtraction and maximal projection of the Z-series images

coactivator may promote mitochondrial uncoupling and thus reduce ΔΨ$_m$ through the induction of the UCPs (Figures 1a and 3a) Thus, we applied quantitative imaging of mitochondrial ΔΨ$_m$ in control and PGC-1α-overexpressing HeLa cells. Cells were loaded with the potential sensitive dye tetramethyl-rhodamine-methyl-ester (TMRM, 20 nM), and the steady-state intensity of the dye accumulated in the mitochondria was measured by confocal imaging. PGC-1α-overexpressing cells (cotransfected with GFP) showed a small (~4%) decrease of TMRM loading compared to controls (mean fluorescence intensity (AU): 1812 ± 16 in control, GFP-expressing cells *versus* 1731 ± 17 in PGC-1α + GFP-expressing cells, $P < 0.01$, Figure 4f). Since the MCU shows a steep voltage dependency,[7] even a small reduction of ΔΨ$_m$ may contribute to the observed reduction of mitochondrial Ca²⁺ uptake kinetics. However, it is unlikely that it fully accounts for the important inhibition of mitochondrial Ca²⁺ uptake caused by PGC-1α overexpression in HeLa cells. Thus, other effects of the transcriptional coactivator on the mitochondrial Ca²⁺ uptake machinery might be responsible for these changes (e.g. downregulation of the yet unidentified Ca²⁺ uniporter).

PGC-1α overexpression protects against Ca²⁺-mediated cell death

Mitochondrial Ca²⁺ uptake has been shown to be a fundamental factor in the activation of the intrinsic apoptotic pathway and in sensitizing the response to several apoptotic stimuli (for recent reviews see Duchen,[24] Rizzuto et al.[25] and Orrenius et al.[26]). Reduction of mitochondrial Ca²⁺ accumulation by PGC-1α thus might result in diminished cellular sensitivity to Ca²⁺-mediated apoptosis. Therefore, we applied C₂ ceramide to induce apoptosis in HeLa cells, as it acts through mitochondrial Ca²⁺ overload and activation of the intrinsic apoptotic pathway following Ca²⁺ release from the ER.[6,27] HeLa cells were transiently transfected with mitochondrially targeted DsRed alone (mtDsRed, controls) or in combination with PGC-1α (PGC-1α-overexpressing

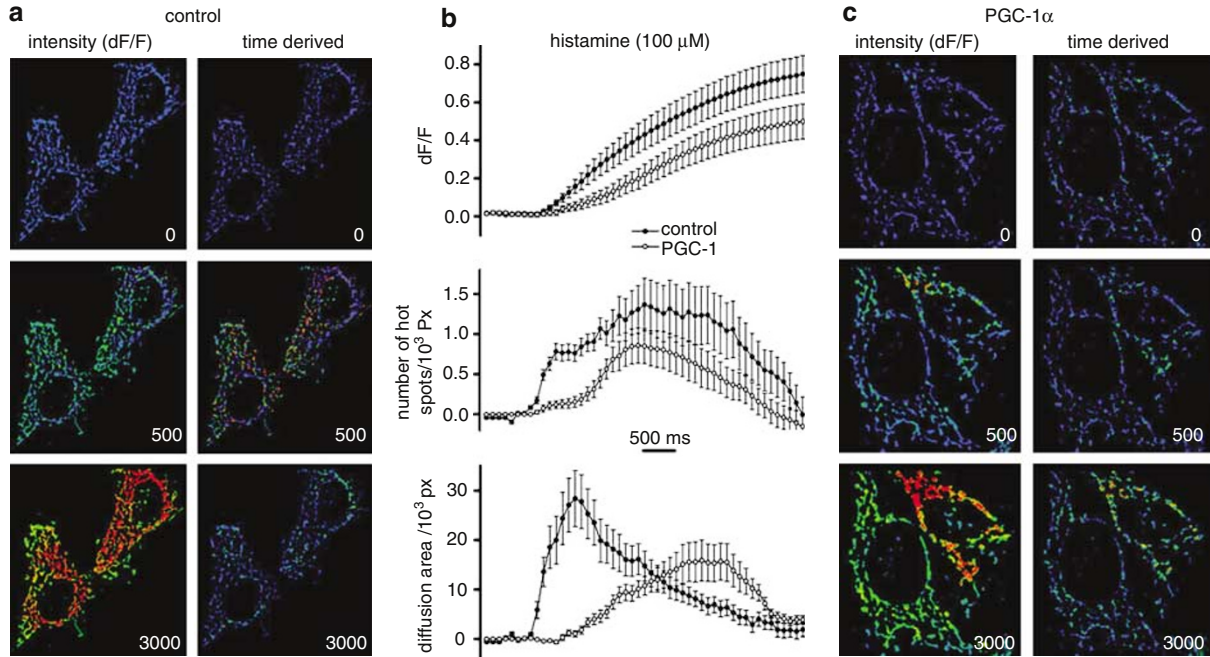**Figure 5** Effect of PGC-1α overexpression on mitochondrial Ca²⁺ uptake and intramitochondrial Ca²⁺ diffusion. HeLa cells were transiently transfected with the mitochondrially targeted Ca²⁺-sensitive ratiometric pericam probe (2mtRP:[40] controls, (**a**) or cotransfected with 2mtRP and PGC-1α (PGC-1α-overexpressing cells, (**c**)). Mitochondrial Ca²⁺ uptake following 100 μM histamine stimulation was imaged at a rate of 5 frames/s. An image mask acquired from 2D image deconvolution was applied to the image series, and relative intensity changes (dF/F, left panels) and velocity of dF (dF/dt, time-derived images, right panels) were calculated (see also Materials and Methods). The former represent the kinetics of Ca²⁺ uptake into the mitochondria, while the latter shows the points of high-velocity [Ca²⁺] changes in the mitochondrial network, that is, 'hot spots' of activation of the MCU.[9] Elapsed time (ms) is indicated on the images. (**b**) Quantitative analysis of Ca²⁺ uptake kinetics from nine cells from three different experiments (mean ± S.E.M.). The upper panel shows the 2mtRP intensity changes during histamine stimulation representing a slower kinetics of Ca²⁺ uptake in PGC-1α-overexpressing cells. The middle panel shows the normalized number of hot spots of Ca²⁺ uptake, initially reduced in PGC-1α-overexpressing cells. The lower panel shows the area of diffusion of Ca²⁺ in the mitochondrial network, which is in contrast to the above parameters is increased in the late phase of mitochondrial Ca²⁺ uptake in PGC-1α-overexpressing cells

cells) and 24 h after transfection the cells were treated with 10 μM C₂ ceramide (10 μM). After overnight incubation with C₂ ceramide and elimination of dead cells we observed a substantial increase in the proportion of PGC-1α-expressing cells after treatment (25.0 ± 8.6% increase in PGC-1α/mtDsRed-overexpressing cells *versus* −2.0 ± 1.6% in control/mtDsRed-expressing cells, $P < 0.05$, Figure 6a). In this experimental setup positive changes in the percentage of surviving transfected cells indicates protection against the apoptotic stimulus by the overexpressed protein, while reduction provides evidence for its proapoptotic effect,[9] thus PGC-1α protected a significant number of cells from C₂ ceramide-induced apoptosis. Moreover, the effect was specific to mitochondrial Ca²⁺-mediated apoptotic stimuli, since no increase in the survival of PGC-1α/mtDsRed-expressing cells was observed when apoptosis was induced by staurosporine, which activates the intrinsic apoptotic pathway in a largely independent way of mitochondrial Ca²⁺ uptake.

These data were confirmed by quantifying nuclear condensation after Hoechst staining, representing and earlier phase of the apoptotic process. Cells were cotransfected with GFP and PGC-1α (PGC-1α-overexpressing cells). Cell death was induced by 40 μM C₂ ceramide and 1 μM staurosporine. After 3 h of treatment, cells were fixed, and the intensity of Hoechst-stained nuclei were quantified in transfected (GFP + PGC-1α) and nontransfected cells. Hoechst intensity was significantly lower in PGC-1α-expressing cells, showing a specific protection against the apoptotic process (1070 ± 62 in PGC-1α/GFP-positive *versus* 1263 ± 60 in nontransfected cells, $P < 0.05$, Figure 6b and c). Interestingly, while staurosporine induced a stronger nuclear condensation, PGC-1α-expressing cells were partially protected in this phase of staurosporine-induced cell death (1620 ± 71 in PGC-1α/GFP-positive *versus* 1785 ± 45 in nontransfected cells, $P = 0.05$).

These results provided evidence that the PGC-1α-induced reduction of mitochondrial Ca²⁺ uptake increases the threshold for Ca²⁺-mediated apoptosis. This compound effect of PGC-1α provides a protective mechanism under stress conditions leading to Ca²⁺ mobilization and Ca²⁺-mediated mitochondrial damage.

Discussion

In the past few years, mitochondria emerged as a central target of several cellular signalling routes including Ca²⁺, apoptotic/necrotic and proliferative signalling pathways, determining cellular function and fate. Here we describe the mechanism by which the transcriptional coactivator PGC-1α, by inducing mitochondrial biogenesis and through direct inhibition of mitochondrial Ca²⁺ uptake modulates Ca²⁺ signalling and cellular apoptotic sensitivity.

The site of PGC-1α action on Ca^{2+} homeostasis

PGC-1α was originally identified as peroxisome-proliferator-activated-receptor-γ (PPAR-γ) coactivator, responsible for adaptive thermogenesis by activating a complex transcriptional programme that leads to increased mitochondrial biogenesis and respiration,[17] and was thus identified as a mitochondrial 'master gene'. Further studies showed that it elicits a pleiotropic effect on metabolism and cellular differentiation including hepatic gluconeogenesis,[28] fatty acid oxida-

tion[29] and type switch of muscle fibres,[30] effects comprising also extramitochondrial processes. Our finding that PGC-1α-overexpressing cells display a change in global cellular Ca^{2+} signalling may reflect these effects; however, the large reduction of mitochondrial Ca^{2+} accumulation together with the observed robust mitochondrial biogenesis rather points to a primary alteration in mitochondrial Ca^{2+} handling. This is further suggested by the fact that FCCP, a protonophore that suppresses $\Delta\Psi_m$ and consequently Ca^{2+} uptake, also reduced the $[Ca^{2+}]_c$ elevation upon histamine challenge. Thus, reduced mitochondrial Ca^{2+} accumulation appears to cause a diminished cytosolic Ca^{2+} signal in HeLa cells. One likely mechanism for this is the well-known phenomenon of local feedback inhibition of Ca^{2+} release from the type 1 IP$_3$R, occurring already at concentrations above 1 μM. Considering that in the Ca^{2+} microdomains between ER and mitochondria of HeLa cells $[Ca^{2+}]$ reaches at least 3–4 μM,[31] any additional Ca^{2+} accumulation is expected to further inhibit the IP$_3$R. Indeed, fast single cell measurement of the cytosolic Ca^{2+} upstroke and population measurements of histamine-induced Ca^{2+} release from the ER confirmed this hypothesis. Reduction of mitochondrial Ca^{2+} uptake led to a faster initial (<1 s) increase of $[Ca^{2+}]_c$ in PGC-1α-overexpressing cells, which in turn caused inhibition of IP$_3$-mediated Ca^{2+} release, slower emptying of the ER and lower $[Ca^{2+}]_c$ response (see Figure 4). In contrast, the cytosolic Ca^{2+} transients in skeletal muscles were not affected by PGC-1α overexpression. This can be assumed to the compound cytosolic Ca^{2+} response of myotubes originating both from Ca^{2+} influx and Ca^{2+} release. Moreover, inactivation of ryanodine receptors starts only at around 50–100 μM $[Ca^{2+}]$.[32] Thus, the Ca^{2+} increase caused by the reduction of mitochondrial Ca^{2+} uptake in the vicinity of ryanodine receptor may well be insufficient to inhibit channel activity.

The mechanism of PGC-1α-induced reduction of mitochondrial Ca^{2+} uptake

Our experiments revealed two principal sites of action of PGC-1α on mitochondrial Ca^{2+} homeostasis. First, it inhibits mitochondrial Ca^{2+} uptake, as evidenced by the reduction in the kinetics of the mitochondrial Ca^{2+} signal and the consequent feedback reduction of ER Ca^{2+} release and
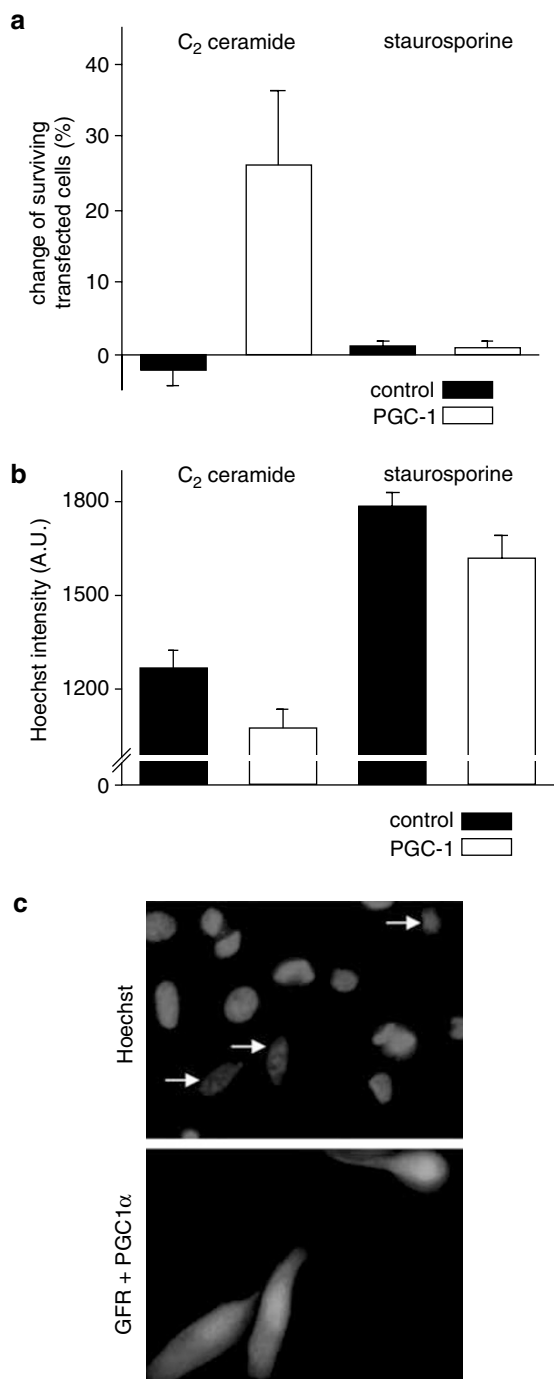
Figure 6 PGC-1α induced mitochondrial biogenesis protects selectively against Ca^{2+} mediated apoptosis. (**a**) Cell death of control and PGC-1α overexpressing HeLa cells was measured by transiently transfecting cells with mitochondrial DsRed (mtDsRed, control cells) and mtDsRed with PGC-1α, and exposing them to C$_2$ ceramide (10 μM, 12 h) and staurosporine (1 μM, 5 h). The histogram shows relative changes of the percentage of surviving transfected cells after C$_2$ ceramide (on the left) and staurosporine (on the right) treatment compared to non-treated cells. Positive values of PGC-1α overexpressing cells represent protection against C$_2$ ceramide induced apoptosis. Data are representative of 6 different experiments, $P<0.05$. (**b**) Quantitative analysis of apoptotic nuclear condensation after 3 h of C$_2$ ceramide (80 μM) and staurosporine (1 μM) treatment. Cells were fixed and nuclei were stained with Hoechst 33342 dye. Figure shows Hoechst intensity measured after backround subtraction on maximal projected Z-series images (see Materials and Methods) (**c**) Representative images of control (non-transfected) and GFP + PGC-1α co-transfected HeLa cells. Nuclei of PGC-1α overexpressing cells (shown by GFP, lower panel) are indicated by arrows on Hoechst images (upper panel)

$[Ca^{2+}]_c$ response. In skeletal myotubes, PGC-1α promotes both coupled and uncoupled respiration.[33] The first is due to the coordinated upregulation of mitochondrial respiratory chain and F_1F_0–ATPase complexes and the second to an increased expression of UCP-2. By promoting the entry of protons into the mitochondrial matrix, UCPs lower mitochondrial potential and thus reduce the driving force for mitochondrial Ca^{2+} influx. This mechanism provides a logical explanation for the reduced mitochondrial Ca^{2+} accumulation in skeletal muscle cells. Nevertheless in HeLa cells we observed a relatively small $\Delta\Psi_m$ reduction, suggesting that overexpression of UCPs do not contribute considerably to the observed inhibitory effect. (However, it should be remembered that Ca^{2+} fluxes through the MCU show a very steep dependence on $\Delta\Psi_m$.) Thus, a possible explanation is that among the numerous gene products regulated by PGC-1α some are part of the mitochondrial Ca^{2+} uptake machinery. Further studies are needed to identify these potential targets of PGC-1α.

The second, indirect mechanism by which PGC-1α reduced the $[Ca^{2+}]$ achieved during the cellular Ca^{2+} signal is the increase of mitochondrial volume. In principle, this volume increase might lead to increased contact surface between mitochondria and ER. However, the digital imaging analysis of the mitochondrial Ca^{2+} transient showed that PGC-1α overexpression does not increase the functionally active Ca^{2+} uptake sites, as we observed a lower number of 'hot spots' during the whole period of mitochondrial Ca^{2+} uptake (see Figure 5). This mechanism thus allows to distribute the Ca^{2+} entered into the mitochondrial matrix in a larger space. Previously we have shown that intramitochondrial Ca^{2+} diffusion is necessary to reach the maximal Ca^{2+} load in the continuous mitochondrial network as fragmentation of mitochondrial network reduced the overall mitochondrial Ca^{2+} load.[9] In this study, we have shown that the opposite change, that is, that the expansion of space between Ca^{2+} uptake sites leads to a similar reduction of the $[Ca^{2+}]_m$ peak/plateau. These studies, together with two recent observations showing that perinuclear clustering of mitochondria modifies the capacitative Ca^{2+} influx[10] and that changes in mitochondrial movements regulates Ca^{2+} uptake in the organelle[34] provide strong evidence that the morphological plasticity of the mitochondrial network is an important regulatory component of the mitochondrial and cellular Ca^{2+} signalling.

PGC-1α regulates cellular sensitivity to apoptosis

Permeabilization of the outer mitochondrial membrane and consequent release of proapoptotic factors from the mitochondrial intermembrane space is an essential component of the intrinsic apoptotic pathway and serve also as an amplification loop in the extrinsic pathway (for recent reviews see Bianchi *et al.*[12], Orrenius *et al.*[26], Green and Kroemer[35] and Hajnoczky *et al.*[36]). The recent progress in exploring the fine regulation of these processes has identified organellar Ca^{2+} content as a key regulatory factor, intertwined at different levels with the apoptosis activatory cascades. Particularly, ER Ca^{2+} content, Ca^{2+} release from the ER and subsequent mitochondrial Ca^{2+} overload was shown to be a key trigger of OMM permeabilization. Ca^{2+} dependency was demonstrated in various apoptotic routes, such as those triggered by serum deprivation, oxidative stress and C_2 ceramide-induced cell death processes. Along these lines, regulatory factors of ER-mitochondrial Ca^{2+} signal transmission axis emerged also as apoptosis regulators. First, pro- and antiapoptotic Bcl-2 family members were shown to increase and decrease, respectively, the ER Ca^{2+} content and Ca^{2+} release. Caspase-8-induced cleavage of the ER membrane resident BAP31 protein leads similarly to Ca^{2+} release and mitochondrial Ca^{2+} overload. The role of mitochondria in these processes was demonstrated by pharmacological tools,[37] but physiological regulation of mitochondrial Ca^{2+} uptake and Ca^{2+} content has not yet been described. We have previously shown that fragmentation of the mitochondrial network, which often accompanies the apoptotic process, reduces its Ca^{2+} load, protecting cells from Ca^{2+}-dependent apoptotic stimuli, however, the cellular regulation of this process is still under investigation. In the present work, we show that PGC-1α-induced mitochondrial changes accomplishes a strict physiological regulation of mitochondrial Ca^{2+} accumulation and consequently also of the Ca^{2+}-dependent apoptotic process. Staurosporine-induced cell death was also shown to be partially inhibited in Bax/Bak-deficient cells,[38] showing reduced steady-state $[Ca^{2+}]_{er}$ and Ca^{2+} release. In our system, PGC-1α presumably protected HeLa cells against staurosporine-induced early apoptosis by interfering with this Ca^{2+}-dependent component of the intrinsic apoptotic pathway.

The transcriptional regulation achieved by the interaction of PGC-1α with PPAR-γ has been shown to be involved in regulating cellular differentiation in different cell types. Moreover, PGC-1α-regulated mitochondrial and extramitochondrial processes play an important role in the adaptation of cellular phenotype to environmental and metabolic changes such as cold exposure and fasting. Along these lines, two recent important observation identified PGC-1α also as a regulator of cell death: the loss of the protein led to loss of striatal function in the brain[18] and its downregulation was shown to be responsible for apoptosis of cardiac myocytes.[20] A likely mechanism for this protection could be the known upregulation of UCPs by PGC-1α, and the consequent downregulation of mitochondrial ROS production, however, no direct experimental evidence supports such a role of PGC-1α in the above pathological models.

In conclusion, we demonstrate that the complex programme activated by PGC-1α (mitochondrial biogenesis and modification of the protein repertoire of the organelle) modifies the responsiveness of mitochondria to cellular Ca^{2+} signals, and thus tunes Ca^{2+}-dependent organelle functions, such as the sensitivity to apoptotic stimuli. This novel mechanism may represent the basis of some of the recently identified effects of PGC-1α (e.g. neuro- and cardiac protection) and the site of pharmacological intervention. The latter possibility, and the crosstalk with other signalling routes or pathophysiological events (e.g. ROS production) will be the subject of further studies.

Materials and Methods

Cell culture and transfection

Primary cultures of skeletal myotubes were prepared from newborn rats as previously described.[39] HeLa cells were kept in DMEM, supplemented

with 10% FCS and seeded onto uncoated glass coverslips. Both cell types were transfected using the Ca^{2+} phosphate technique, 24 h (HeLa) or 48 h (myoblasts) after plating. Myotubes were differentiated on the day after transfection by replacing the incubation medium with DMEM containing 2% HS. For luminescence measurements, cells were transfected with 1 μg of the differentially targeted aequorins (cytosolic: cytAEQ, mitochondrial: mitAEQmut, ER: erAEQmut, SR: srAEQmut[22] alone (controls), or with 3 μg of human PGC-1α in pcDNA4/TO. After overnight incubation, cells were washed thoroughly with PBS and myoblasts were grown in DMEM supplemented with 2% horse serum to allow myotube formation.

Aequorin measurements

CytAEQ-, mtAEQmut- or erAEQmut-expressing cells were reconstituted with coelenterazine, transferred to the perfusion chamber, light signal was collected in a purpose-built luminometer and calibrated into $[Ca^{2+}]$ values as previously described.[22] All aequorin measurements were carried out in KRB containing 1 mM $CaCl_2$ (KRB/Ca^{2+}, Krebs–Ringer modified Buffer: 135 mM NaCl, 5 mM KCl, 1 mM $MgSO_4$, 0.4 mM K_2HPO_4, 1 mM $CaCl_2$, 5.5 mM glucose, 20 mM HEPES, pH = 7.4).

Imaging procedures

For $[Ca^{2+}]_c$ imaging, cells were loaded with 4 μM fura-2 AM for 30 min at 37°C in KRB/Ca^{2+} solution. Cells were imaged using an inverted Zeiss Axiovert 200 M microscope (Carl Zeiss, Jena, Germany) using a 40 × /1.3/ oil Fluar objective. Fura-2 fluorescence was measured at 340 and 380 nm excitation using a random access monochromator (Photon Technology International, NJ, USA) and emission was detected using a 505/30 emission filter. Images at 20–40 frame/s were acquired with a 512BFT Cascade camera (Princeton Instruments, AZ, USA) at 37°C. Analysis was carried out using the MetaFluor Analyst software (Universal Imaging Corporation, PA, USA).

For $[Ca^{2+}]_m$ imaging, HeLa cells were transiently transfected with the mitochondrially targeted Ca^{2+}-sensitive ratiometric pericam probe (2mtRP[40]) ± PGC-1α. After 36 h of transfection, cells were placed in a thermostatted chamber at 37°C in KRB/Ca^{2+}. Cells were imaged using an inverted Zeiss Axiovert 200 M microscope (Carl Zeiss, Jena, Germany) using a 63 × /1.4/oil Plan-Apochromat objective. The 2mtRP probe was excited at 410 nm, using a random access monochromator (Photon Technology International, NJ, USA) and imaged with the 512BFT Cascade intensified camera at 20 frame/s. The first raw image of the time series was deconvolved using the no-neighbours algorithm (MetaMorph 5.0, Universal Imaging), and thresholded to create a binary mask. The mask was applied to dF/F images, calculated from the raw image series. Time-derived images were calculated using the MetaFluor Analyst software of the Meta Imaging software package (Universal Imaging). Images were then transformed to a MetaMorph stack file, thresholded and subjected to integrated morphology analysis. Hot spots and diffusion area were calculated as total area of separated objects over a standard threshold applied for all images.

For 3D image acquisition the cells were transfected with mtGFP. Cells were imaged at 20°C using an inverted Zeiss Axiovert 200 M microscope (Carl Zeiss, Jena, Germany) using a 63 × /1.4/oil Plan-Apochromat objective, a CoolSNAP$_{HQ}$ interline CCD camera (Roper Scientific, NJ, USA) and the MetaMorph 5.0 software (Universal Imaging Corporation, PA, USA). Z-series images were deconvolved using the PSF-based Exhaustive Photon Reassignment deconvolution software,[41,42] running on a Linux-based PC. For volume analysis the custom-made Data Analysis And Visualization Environment (DAVE) software was used.[42]

For measurement of $\Delta\Psi_m$ cells were loaded with 10 nM TMRM for 30 min at 37°C and steady-state intensity of the dye was quantified as previously described.[9]

For quantifying nuclear condensation, cells were cotransfected with GFP and PGC-1α. After 3 h of C_2 ceramide (40 μM) or staurosporine (1 μM) treatment, cells were fixed (4% *p*-formaldehyde) and stained with 2 μM Hoechst 33342 for 30 min at 37°C. Z-series of digital images were acquired (see above) at 360 nm (Hoechst) and 485 nm (GFP), and intensity was quantified on maximal projection images after background correction using the MetaMorph software (Universal Imaging Corporation, PA, USA).

Western blot and immunofluorescence analysis

HeLa cells and primary myotubes were plated in 35 mm well plates. After PGC-1α expression or salbutamol treatment cells were washed twice in PBS, trypsinized, pelleted (1000 rpm, 5 min, RT), resuspended and homogenized (10 mM NaCl, 10 mM Tris-HCl, 1 mM EDTA, 1 mM EGTA, 1 mM DTT, protease inhibitor cocktail [Sigma-Aldrich], pH 7.4). Proteins were separated by SDS-PAGE on a 10% gel, and the amount of PGC-1α, UCP-2, NRF-1 and β-tubulin was estimated by Western blotting using polyclonal rabbit anti-PGC-1α (1 : 5000) goat anti-UCP-2 (1 : 3000) goat anti-NRF-1 (1 : 200) and monoclonal mouse anti-β-tubulin (1 : 5000) primary antibodies and respective HRP-labeled secondary antibodies (1 : 5000), according to standard protocols. All antibodies were from Santa-Cruz Biotechnologies, CA, USA. Immunofluorescence analysis was performed as previously described,[43] using the polyclonal rabbit anti-PGC-1α (1 : 500) PGC-1α primary antibody, followed by the visualization with the AlexaFluor 549 anti-rabbit antibody (Invitrogen, Molecular Probes™).

Data analysis

All data are expressed as mean ± S.D. unless otherwise stated. Where appropriate, the Student's *t*-test was used for statistical evaluation.

Acknowledgements

References

1. Berridge MJ, Bootman MD and Roderick HL (2003) Calcium signalling: dynamics, homeostasis and remodelling. Nat. Rev. Mol. Cell Biol. 4: 517–529
2. Rizzuto R, Duchen MR and Pozzan T (2004) Flirting in little space: the ER/mitochondria Ca²⁺ liaison. Sci. STKE. 2004 (215): re1
3. Parekh AB (2003) Store-operated Ca²⁺ entry: dynamic interplay between endoplasmic reticulum, mitochondria and plasma membrane. J. Physiol. 547: 333–348
4. Gunter TE, Yule DI, Gunter KK, Eliseev RA and Salter JD (2004) Calcium and mitochondria. FEBS Lett. 567: 96–102

5. McCormack JG, Halestrap AP and Denton RM (1990) Role of calcium ions in regulation of mammalian intramitochondrial metabolism. Physiol. Rev. 70: 391–425

6. Szabadkai G and Rizzuto R (2004) Participation of endoplasmic reticulum and mitochondrial calcium handling in apoptosis: more than just neighborhood? FEBS Lett. 567: 111–115

7. Kirichok Y, Krapivinsky G and Clapham DE (2004) The mitochondrial calcium uniporter is a highly selective ion channel. Nature 427: 360–364

8. Gincel D, Zaid H and Shoshan-Barmatz V (2001) Calcium binding and translocation by the voltage-dependent anion channel: a possible regulatory mechanism in mitochondrial function. Biochem. J. 358: 147–155

9. Szabadkai G, Simoni AM, Chami M, Wieckowski MR, Youle RJ and Rizzuto R (2004) Drp-1 dependent division of the mitochondrial network blocks intraorganellar Ca^{2+} waves and protects against Ca^{2+} mediated apoptosis. Mol. Cell. 16: 59–68

10. Frieden M, James D, Castelbou C, Danckaert A, Martinou JC and Demaurex N (2004) Ca(2+) homeostasis during mitochondrial fragmentation and perinuclear clustering induced by hFis1. J. Biol. Chem. 279: 22704–22714

11. Karbowski M and Youle RJ (2003) Dynamics of mitochondrial morphology in healthy cells and during apoptosis. Cell Death Differ. 10: 870–880

12. Bianchi K, Rimessi A, Prandini A, Szabadkai G and Rizzuto R (2004) Calcium and mitochondria: mechanisms and functions of a troubled relationship. Biochim. Biophys. Acta. 1742: 119–131

13. Scarpulla RC (2002) Transcriptional activators and coactivators in the nuclear control of mitochondrial function in mammalian cells. Gene 286: 81–89

14. Puigserver P and Spiegelman BM (2003) Peroxisome proliferator-activated receptor-gamma coactivator 1 alpha (PGC-1 alpha): transcriptional coactivator and metabolic regulator. Endocr. Rev. 24: 78–90

15. Schaeffer PJ, Wende AR, Magee CJ, Neilson JR, Leone TC, Chen F and Kelly DP (2004) Calcineurin and calcium/calmodulin-dependent protein kinase activate distinct metabolic gene regulatory programs in cardiac muscle. J. Biol. Chem. 279: 39593–39603

16. Wu H, Kanatous SB, Thurmond FA, Gallardo T, Isotani E, Bassel-Duby R and Williams RS (2002) Regulation of mitochondrial biogenesis in skeletal muscle by CaMK. Science 296: 349–352

17. Puigserver P, Wu Z, Park CW, Graves R, Wright M and Spiegelman BM (1998) A cold-inducible coactivator of nuclear receptors linked to adaptive thermogenesis. Cell 92: 829–839

18. Lin J, Wu PH, Tarr PT, Lindenberg KS, St Pierre J, Zhang CY, Mootha VK, Jager S, Vianna CR, Reznick RM, Cui L, Manieri M, Donovan MX, Wu Z, Cooper MP, Fan MC, Rohas LM, Zavacki AM, Cinti S, Shulman GI, Lowell BB, Krainc D and Spiegelman BM (2004) Defects in adaptive energy metabolism with CNS-linked hyperactivity in PGC-1alpha null mice. Cell 119: 121–135

19. Garnier A, Fortin D, Delomenie C, Momken I, Veksler V and Ventura-Clapier R (2003) Depressed mitochondrial transcription factors and oxidative capacity in rat failing cardiac and skeletal muscles. J. Physiol. 551: 491–501

20. Sano M, Wang SC, Shirai M, Scaglia F, Xie M, Sakai S, Tanaka T, Kulkarni PA, Barger PM, Youker KA, Taffet GE, Hamamori Y, Michael LH, Craigen WJ and Schneider MD (2004) Activation of cardiac Cdk9 represses PGC-1 and confers a predisposition to heart failure. EMBO J. 23: 3559–3569

21. Wu Z, Puigserver P, Andersson U, Zhang C, Adelmant G, Mootha V, Troy A, Cinti S, Lowell B, Scarpulla RC and Spiegelman BM (1999) Mechanisms controlling mitochondrial biogenesis and respiration through the thermogenic coactivator PGC-1. Cell 98: 115–124

22. Chiesa A, Rapizzi E, Tosello V, Pinton P, de Virgilio M, Fogarty KE and Rizzuto R (2001) Recombinant aequorin and green fluorescent protein as valuable tools in the study of cell signalling. Biochem. J. 355: 1–12

23. Rapizzi E, Pinton P, Szabadkai G, Wieckowski MR, Vandecasteele G, Baird G, Tuft RA, Fogarty KE and Rizzuto R (2002) Recombinant expression of the voltage-dependent anion channel enhances the transfer of Ca^{2+} microdomains to mitochondria. J. Cell Biol. 159: 613–624

24. Duchen MR (2004) Mitochondria in health and disease: perspectives on a new mitochondrial biology. Mol. Aspects Med. 25: 365–451

25. Rizzuto R, Pinton P, Ferrari D, Chami M, Szabadkai G, Magalhaes PJ, Di Virgilio F and Pozzan T (2003) Calcium and apoptosis: facts and hypotheses. Oncogene 22: 8619–8627

26. Orrenius S, Zhivotovsky B and Nicotera P (2003) Regulation of cell death: the calcium-apoptosis link. Nat. Rev. Mol. Cell Biol. 4: 552–565

27. Pinton P, Ferrari D, Rapizzi E, Di Virgilio FD, Pozzan T and Rizzuto R (2001) The Ca^{2+} concentration of the endoplasmic reticulum is a key determinant of ceramide-induced apoptosis: significance for the molecular mechanism of Bcl-2 action. EMBO J. 20: 2690–2701

28. Yoon JC, Puigserver P, Chen G, Donovan J, Wu Z, Rhee J, Adelmant G, Stafford J, Kahn CR, Granner DK, Newgard CB and Spiegelman BM (2001) Control of hepatic gluconeogenesis through the transcriptional coactivator PGC-1. Nature 413: 131–138

29. Wang YX, Lee CH, Tiep S, Yu RT, Ham J, Kang H and Evans RM (2003) Peroxisome-proliferator-activated receptor delta activates fat metabolism to prevent obesity. Cell 113: 159–170

30. Lin J, Wu H, Tarr PT, Zhang CY, Wu Z, Boss O, Michael LF, Puigserver P, Isotani E, Olson EN, Lowell BB, Bassel-Duby R and Spiegelman BM (2002) Transcriptional co-activator PGC-1 alpha drives the formation of slow-twitch muscle fibres. Nature 418: 797–801

31. Csordas G, Thomas AP and Hajnoczky G (1999) Quasi-synaptic calcium signal transmission between endoplasmic reticulum and mitochondria. EMBO J. 18: 96–108

32. Meissner G (2002) Regulation of mammalian ryanodine receptors. Front Biosci. 7: d2072–d2080

33. Wu H, Kanatous SB, Thurmond FA, Gallardo T, Isotani E, Bassel-Duby R and Williams RS (2002) Regulation of mitochondrial biogenesis in skeletal muscle by CaMK. Science 296: 349–352

34. Yi M, Weaver D and Hajnoczky G (2004) Control of mitochondrial motility and distribution by the calcium signal: a homeostatic circuit. J. Cell Biol. 167: 661–672

35. Green DR and Kroemer G (2004) The pathophysiology of mitochondrial cell death. Science 305: 626–629

36. Hajnoczky G, Davies E and Madesh M (2003) Calcium signaling and apoptosis. Biochem. Biophys. Res. Commun. 304: 445–454

37. Breckenridge DG, Stojanovic M, Marcellus RC and Shore GC (2003) Caspase cleavage product of BAP31 induces mitochondrial fission through endoplasmic reticulum calcium signals, enhancing cytochrome c release to the cytosol. J. Cell Biol. 160: 1115–1127

38. Scorrano L, Oakes SA, Opferman JT, Cheng EH, Sorcinelli MD, Pozzan T and Korsmeyer SJ (2003) BAX and BAK regulation of endoplasmic reticulum Ca^{2+}: a control point for apoptosis. Science 300: 135–139

39. Cantini M, Massimino ML, Catani C, Rizzuto R, Brini M and Carraro U (1994) Gene transfer into satellite cell from regenerating muscle: bupivacaine allows beta-Gal transfection and expression in vitro and in vivo. In Vitro Cell Dev. Biol. Anim. 30A: 131–133

40. Filippin L, Magalhaes PJ, Di Benedetto G, Colella M and Pozzan T (2003) Stable interactions between mitochondria and endoplasmic reticulum allow rapid accumulation of calcium in a subpopulation of mitochondria. J. Biol. Chem. 278: 39224–39234

41. Carrington WA, Lynch RM, Moore ED, Isenberg G, Fogarty KE and Fay FS (1995) Superresolution three-dimensional images of fluorescence in cells with minimal light exposure. Science 268: 1483–1487

42. Rizzuto R, Carrington W and Tuft RA (1998) Digital imaging microscopy of living cells. Trends Cell Biol. 8: 288–292

43. Chami M, Prandini A, Campanella M, Pinton P, Szabadkai G, Reed JC and Rizzuto R (2004) Bcl-2 and Bax exert opposing effects on Ca^{2+} signaling, which do not depend on their putative pore-forming region. J. Biol. Chem. 279: 54581–54589